JOURNAL OF MATERIALS SCIENCE 27 (1992) 3085–3091

Friction and wear behaviour of continuous fibre as cast Kevlar–phenolic resin composite

S. K. SINHA, S. K. BISWAS
Mechanical Engineering Department, Indian Institute of Science, Bangalore 560012, India

A compression moulded Kevlar–phenolic resin composite consisting of 30 wt% continuous fibres was slid against a steel disc such that the fibre axis was normal to the sliding plane. The sliding experiments were conducted in a normal pressure range of 0.47–4.27 MPa and at a sliding speed of 0.5 $m s^{-1}$. The initial sliding interaction is abrasive. With further sliding, as patches of polymer transfer film develop on the polymer pin and counterface, the interaction becomes adhesive and steady-state friction is established. The wear resistance of the polymer was found to be related to the stability of this film.

1. Introduction

Table I gives an overview of some of the recent studies on the effect of fibre reinforcement of polymers on friction and wear. For most polymers fibre addition lowers the friction coefficient.

Laying aside the effects of fibre orientation (a normal orientation gives the best performance) and fibre percentage, and taking a sweeping view of the published results on the wear resistance of these composites, the size of the fibres appears to have a strong influence on the wear resistance of the composite. The effect of fibre addition on the wear resistance of short-fibre composites appears to depend on the ability of the fibre to accommodate strain; carbon fibre addition improves and glass fibre addition adversely affects the wear resistance. However, when the fibres added are long, the wear resistance of almost all fibre composites improves due to fibre addition. Furthermore, under abrasive conditions continuous-fibre composites [1] appear to register a higher wear resistance than short-fibre composites [2].

Under abrasive and adhesive traction short fibres are pulled out easily by debonding. This weakens the immediate subsurface. The fibres in the process are fractured and in some cases pulverized. When the fibres are made of hard material such as glass, the fibre further abrades the composite. When the fibres are continuous and their axis normally oriented to the sliding plane they are well anchored in the bulk. They are therefore not easy to pull out. Under the machining type of traction, when the fibres are cut or sheared at the tip a part of the traction energy is dissipated in straining the fibre. This may ultimately result in debonding of the fibre from the matrix and bending and fracture of the fibre, but in the process the matrix dissipates a correspondingly smaller amount of energy. This would presumably leave the subsurface relatively undisturbed, giving rise to a high wear resistance. If this mechanism is valid, tough fibres would tend to give the best performance. Considering that the tensile strength of aramid fibres (Kevlar 49) is somewhat higher and the breaking strain is considerably more than for carbon fibres, the aramid fibre composites would be expected to yield better wear resistance than those containing carbon fibres. Under abrasive conditions Cirino *et al.* [1] have indeed shown the wear resistance of normally oriented aramid fibre composite to be about four times that of similarly oriented carbon fibre composite.

To be considered for brake applications a material should satisfy the following requirements [3].

1. Stable or steady-state friction coefficient which is maintained over long usage at a level of about 0.3.
2. Low wear.
3. Load index of the order of unity.
4. Fast pick-up of the steady-state friction level. The steady-state friction level should be reached very soon after the commencement of the braking operation.
5. There should not be a sudden brake failure in the case of leakage of any environmental fluid into the braking interface.

The normal operating pressure for a typical disc pad is around 1 MPa compared with 0.2 MPa for a drum brake lining and 4 MPa for heavy-duty brake application. Typical speeds are 1.9–3.2 $m s^{-1}$.

The present study was a qualitative mechanistic evaluation of the tribology of as-cast aramid fibre composite. The matrix was a phenolic resin and the fibre was Kevlar 49 (axially) oriented normal to the sliding plane. The counterface was a ground steel disc. An attempt is made to understand the tribo-mechanistic changes brought about by fibre addition to the resin. Notwithstanding the relatively low velocity at which the present study was conducted, the discussion section of this paper includes an assessment of the potential of Kevlar–phenolic resin composite as a brake material.

0022–2461

TABLE I

Polymer composite			Effect of fibre inclusion[a]		
Matrix	Fibre		Friction	Wear	Reference
	Short	Continuous			
PEI	GF		(+)	(−)	[4]
PEEK	GF			(+)	[6]
				(+)	[7]
				(+)	[8]
PEEK	CF			(−)	[6]
				(−)	[7]
PBT	CF		(−)		[5]
PBT	GF		(+)	(+)	[5]
				(+)	[9]
PBT	GF	(Water lubricated)		(+)	[9]
PPS		CF	(−)	(−)	[10]
PPS		CF (Water lubricated)	(−)	(−)	[11]
Phenolic resin		Kevlar	(−)		[3]
PEEK		CF	(+)	(+)	[1]
Epoxy		CF		(−)	[1]
				(−)	[12]
Epoxy		Kevlar	(−)	(−)	[1]
and PEEK				(−)	[12]
Nylon		GF (Water lubricated)		(−)	[13]
Epoxy		GF	(+)	(−)	[14]
			(+)	(−)	[12]
Epoxy		CF + GF	(−)	(−)	[12]

Abbreviations: PEI, polyetheramide; PEEK, poly(ether·ether ketone); PBT, poly(butylene terephthalate); PPS, poly(phenylene sulphide); GF, glass fibre; CF, carbon fibre.
[a] (+) increase and (−) decrease.

2. Experimental procedure

2.1. Sample preparation

The composite consisting of 30% fibre and phenolic resin samples were prepared in the laboratory. Phenolic resin was supplied by Bakelite Hylam Ltd, Hyderabad, India, and Kevlar 49 fibre was supplied by The National Aeronautics Laboratory, India. Chemically phenolic resin is a crosslinked structure of phenol formaldehyde. Kevlar fibre is poly(*p*-phenylene terephthalamide), which crystallizes in the monoclinic system with two monomers in the unit cell. The samples were cast by the compression moulding method using a die and punch [3]. Alternate layers of weighed amounts of resin and fibre (30 wt %) were laid over one other in the die cavity of dimensions 20 mm × 30 mm × 30 mm. The material was preheated for 30 min and then pressed at 65 MPa. The sample was cured for 30 h at 180 °C under the pressed condition. It was subsequently cooled in the furnace. Pins of length 20 mm and surface area 20 mm^2 (4 mm × 5 mm) were machined out of the cast block such that the axis of the fibre was parallel to the pin axis. The samples were found to be free of any macrodefects such as voids or cracks. The density of the composite specimen was 1.3 $g\,cm^{-3}$.

2.2. Experimental set-up

Dry sliding and wet sliding (water as lubricant) experiments were done using a pin-on-disc apparatus. The counterface used was EN-24 steel (hardness 55RC) ground to different roughnesses. Friction was measured by strain gauges attached to the arm of the specimen holder and wear was measured using a displacement measuring instrument (LVDT). In the wet sliding experiment a constant stream of water (at room temperature) was poured into the trailing edge of the pin throughout the experiment.

2.3. Testing procedure

Before every experiment the sample surface was prepared by sliding it over an abrasive paper (400-grade) at a normal pressure of 0.12 MPa to ensure good contact (during the actual experiment) between the specimen and the counterface. After this preparatory abrasion the counterface and sample surfaces were cleaned with acetone. The surface speed was maintained at 0.5 $m\,s^{-1}$ while the normal pressure was varied between 0.476 and 4.25 MPa. The reported characteristics are averages from three experiments. The standard deviation of results from three experiments were found to be $\pm$ 0.0489 for the friction coefficient and $\pm\, 6.14 \times 10^{-8}\ mm^3\,mm^{-1}$ for the wear rate. The worn specimens were sectioned parallel to the sliding direction. The exposed planes contained the full length of some fibres. These sections are referred to as parallel sections. Parallel sections and worn surfaces were coated with gold and examined by scanning electron microscopy (SEM).

3. Results

3.1. Friction of the composite material

Fig. 1 shows that up to a normal pressure of 3.77 MPa the friction coefficient increases initially and then remains approximately constant with time. Fig. 2a shows that after initial preparatory abrasion the surface consists of score marks interspersed with spots of morphologically smooth film. These spots of film grow in area with the sliding time (Fig. 2b) in the transient stage. In the steady-state stage the area covered by the film does not increase with the sliding time. The area not covered by the film was found to undergo ductile ploughing, with longitudinal (in the direction of sliding) and transverse cracks joining to yield laminate-type debris. The morphology of the ploughed zone was found to be very similar to that observed when a composite specimen was abraded with emery paper and distinctly different from the predominantly brittle fracture observed when a resin specimen was slid against the steel counterface. Fig. 2c shows the edge of a smooth film with a few microcracks at the edges and the ploughed zone marked by extensive plastic flow and delamination. The transient stage of the friction characteristic is thus predominantly marked by abrasion in the beginning. Abrasion releases debris which appears to be ironed on the pin as well as the counterface as patches of film. Fig. 3 shows that the counterface in the transient stage develops a film which increases in height with time until the counterface asperities are enveloped by the film. This marks the steady-state phase in which the sliding promotes predominantly adhesive interaction between the two films. Thus, the transient stage, which starts off as predominantly abrasive, becomes less abrasive and more adhesive with progressive sliding. The adhesive steady-state phase is marked by a high level of friction.

The nature of interaction at the sliding interface is often revealed by the value of the load index, n, obtained from

$$F = kW^n$$

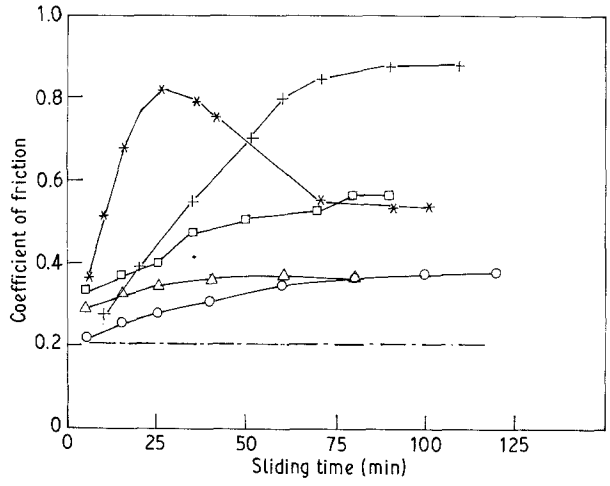

Figure 1 Coefficient of friction of composite against sliding time. (*) 4.25 MPa, 0.05–0.1 μm CLA; (+) 3.77 MPa, 0.05–0.1 μm CLA; (□) 0.476 MPa, 0.05–0.1 μm CLA; (○) 4.25 MPa, 0.3–0.4 μm CLA; (△) 4.25 MPa, 1.0–1.5 μm CLA; (– – –), 4.25 MPa, 0.05–0.1 μm CLA, water lubricated.

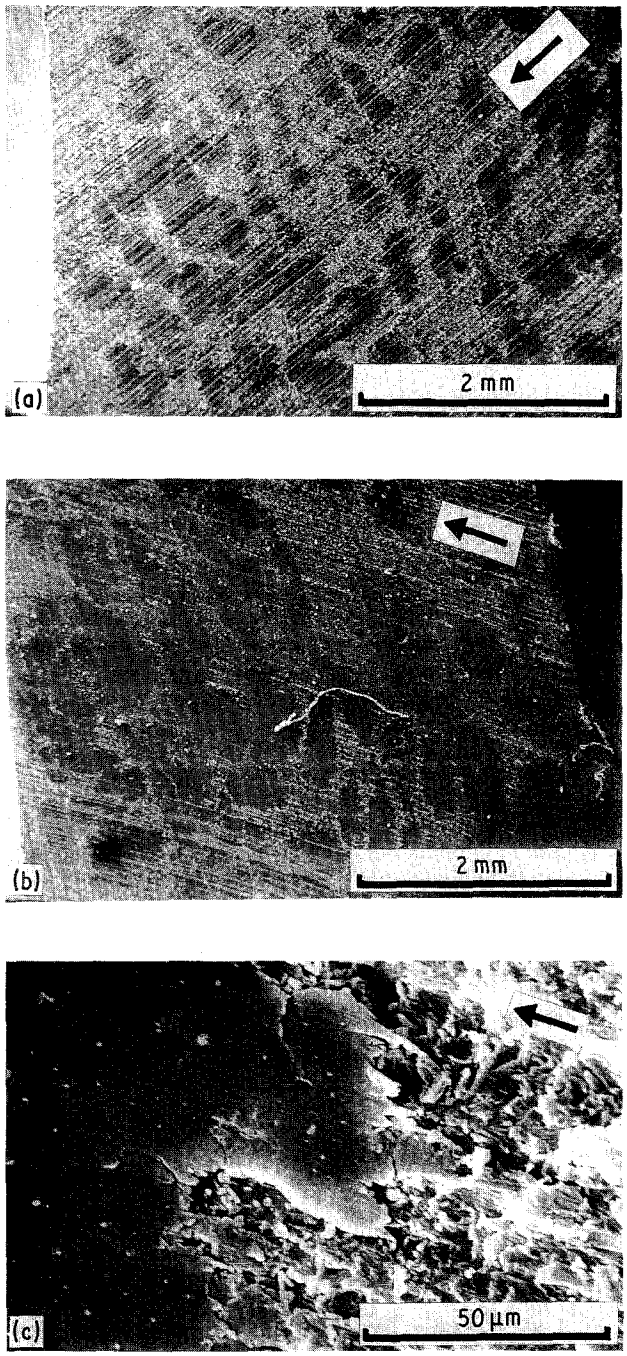

Figure 2 Low-magnification SEM of composite and resin surfaces (arrow indicates sliding direction): (a) composite slid against emery paper at 0.12 MPa, (b) composite slid against steel counterface (0.05–0.1 μm CLA) for 5 min at 3.77 MPa normal pressure and (c) composite slid against steel (0.05–0.1 μm CLA) at 2.04 MPa in steady state.

where F is the friction force and W is the normal load. The load index in the transient stage in the present case was found to be about 0.85, suggesting asperity persistence. The steady-state load index was estimated to be 1.0–1.1, indicating the existence of extensive flow at the contact. The asperity persistence at the transient stage may be associated with the counterface asperities interacting with continuously generated new asperities (on the pin) by the process of abrasion. At the steady-state stage film–film interaction gives rise to flow.

Further proof of the changing nature of interaction between the pin and disc with sliding distance was

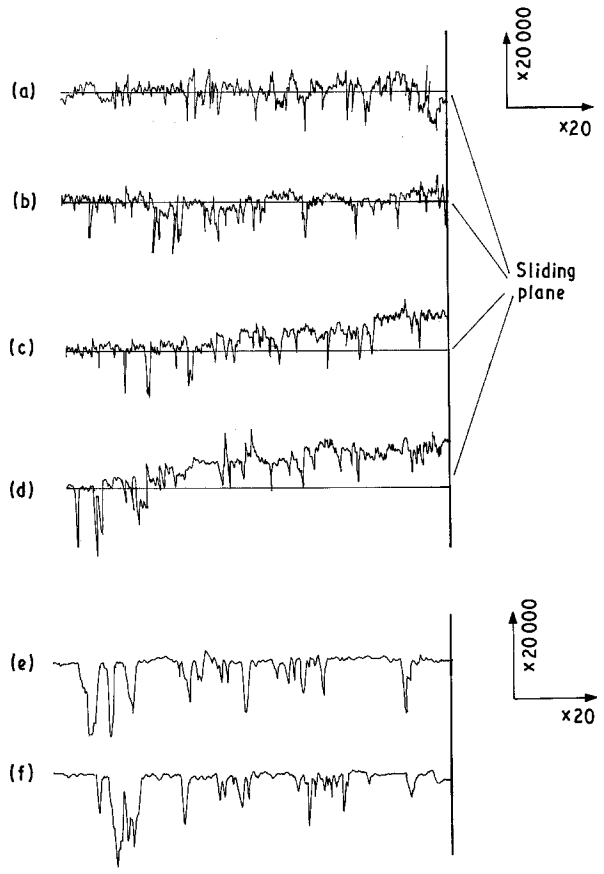

Figure 3 Profilometric traces showing topographical changes with sliding time at the same location of the counterface. Each trace shows a part of the slide and a part of the unslid wear track. Normal pressure 3.77 MPa and counterface roughness 0.05–0.1 μm CLA: (a) original surface, (b) 10 min sliding, (c) 30 min sliding and (d) 60 min sliding. Normal pressure 3.77 MPa and counterface roughness 1.0–1.5 μm CLA: (e) original surface and (f) after 60 min sliding.

obtained by sliding the composite pin against rough counterfaces. Fig. 3e and f shows that when the counterface is rough, even after 60 min sliding, the disc topography remains virtually unchanged. Examination of the pin surface slid against a rough counterface also revealed no film formation. The friction coefficient corresponding to the rough counterface changed little with the sliding time (Fig. 1); the pin–disc interaction in this case may be designated as mainly abrasive and the corresponding level of friction coefficient (0.2–0.3) characteristic of dry abrasion. Considering the fact that the level of friction coefficient achieved when the pin is slid against a smooth (0.05–0.1 μm CLA) counterface is initially (at all pressures) about 0.2–0.3, and that it changes sharply away from that level with further sliding, it is fair to state that although all interaction with the smooth counterface is abrasive initially ($\mu = 0.2$–0.3) it becomes less so progressively with sliding, and finally a predominantly adhesive steady state is achieved in which the friction is independent of the sliding distance, but linearly dependent on the load.

It is interesting to note from Fig. 1 that the friction coefficient first falls and then rises with increasing roughness. The fall may be due to a decrease in the adhesion component and the subsequent rise is due to an increase in the abrasion component. This effect has been noted for other polymer systems rubbing against a hard counterface [4].

3.2. Friction at high normal pressure

At a normal pressure of 4.25 MPa the surface coverage by the polymer film starts to increase rapidly after about 20 min sliding, which marks a slowing down of the rate of increase of the friction coefficient with sliding time (Fig. 1). After about 30 min sliding the temperature at the interface must become sufficiently high to give rise to large-scale melting of the surface layers and a consequent fall in the coefficient of friction, due to the existence of a molten or a semi-molten film at the interface. Fig. 4a shows a pocket of spherical particles found on a 4.25 MPa worn surface. Such particles are typical of melt wear. The surface melting is also accompanied by plasticity of the subsurface. The latter appears to give rise to subsurface cracks, which reach the surface with sliding, yielding large laminate-type debris as seen in Fig. 4b.

3.3. Effect of fibre addition

Fig. 5 shows that the presence of fibres lowers the steady-state friction coefficient considerably. At the onset of sliding the friction coefficient of the resin is about the same as that of the composite. As the sliding time increases, the friction coefficient of the resin rises to levels almost twice that of the composite. Fig. 5 also shows that the addition of fibres delays the achievement of the steady state.

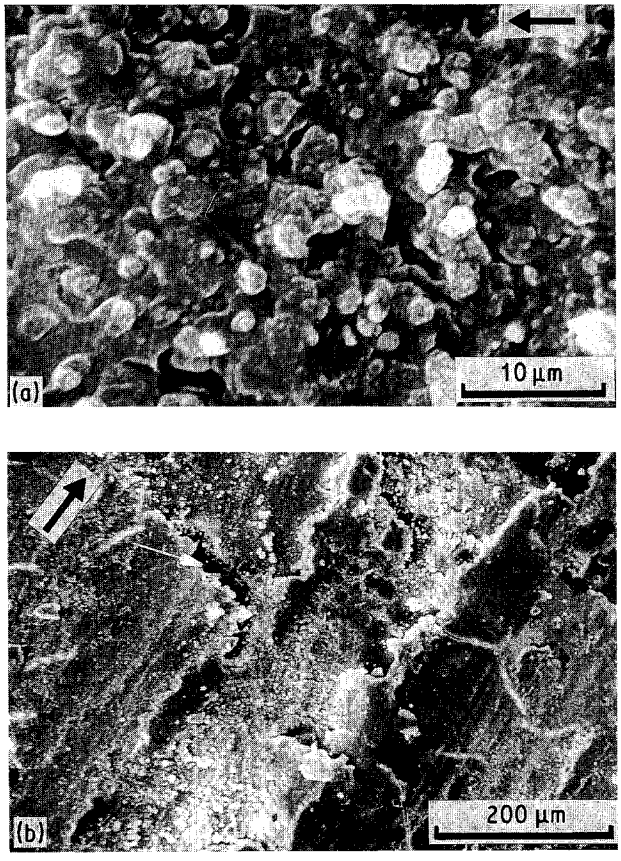

Figure 4 SEM of composite at 4.25 MPa normal pressure in steady state. The white arrow points to laminate debris being released.

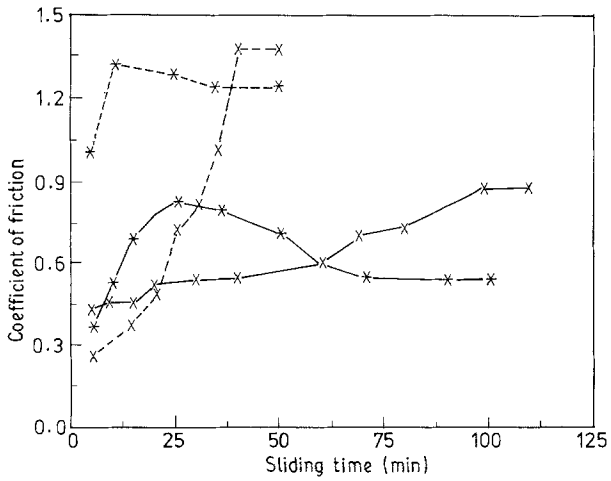

Figure 5 Coefficient of friction against sliding time (counterface roughness 0.05–0.1 μm CLA). Resin (broken curves) and composite (full curves), normal pressure: (*) 4.25 MPa and (×) 2.04 MPa.

3.4. Wear

The initially abraded resin sample surface developed a serrated morphology within a short sliding time (Fig. 6a). Such a morphology suggests [5] a severe stick–slip condition under high adhesion. The weakened surface breaks up when abraded (see deep groove in Fig. 6a), giving rise to a high rate of wear in the transient stage (Fig. 7, 2.04 MPa). The fracture extends to a depth of about 10 μm, as seen in Fig. 6b. With the progress of sliding, patches of film (Fig. 6b) develop on the surface. This stabilizes friction and reduces the wear rate. At a high normal pressure of 4.25 MPa the latter mode is followed by surface melting, which raises the wear rate again (after 50 min sliding) as seen in Fig. 7. The wear rate in the case of the composite remains relatively high as long as the abrasive mode predominates. That the abrasive mode results in a high wear rate is further established by noting (for the composite) the significant jump in wear rate obtained when the counterface roughness is increased from 0.05 to 0.1 μm CLA (Fig. 7).

In the steady state the addition of fibres appears to remove the source of severe adhesion, and low adhesion between smooth stable films on the pin and counterface becomes the predominant interactive mode. Up to 3.77 MPa the composite specimen surface in the steady-state phase undergoes extensive plastic flow. In the absence of the stick–slip mode the surface fracture is greatly reduced if not eliminated. Few cracks in this case emanate from the fibre–matrix interface in the subsurface and propagate on to the surface, giving rise to laminate-type debris (Fig. 8). In the steady state, when the low adhesive interaction between films is established as the predominant mode, the wear rate (possibly only in the delaminative mode) falls to a very low level.

However, as the normal pressure is increased above 3.77 MPa surface melting takes place (Fig. 4) in the steady-state phase, increasing the wear rate of the composite slightly (Fig. 7). It is interesting to note in Fig. 7 that water lubrication actually increases the wear in the case of the composite. Fig. 9 shows the

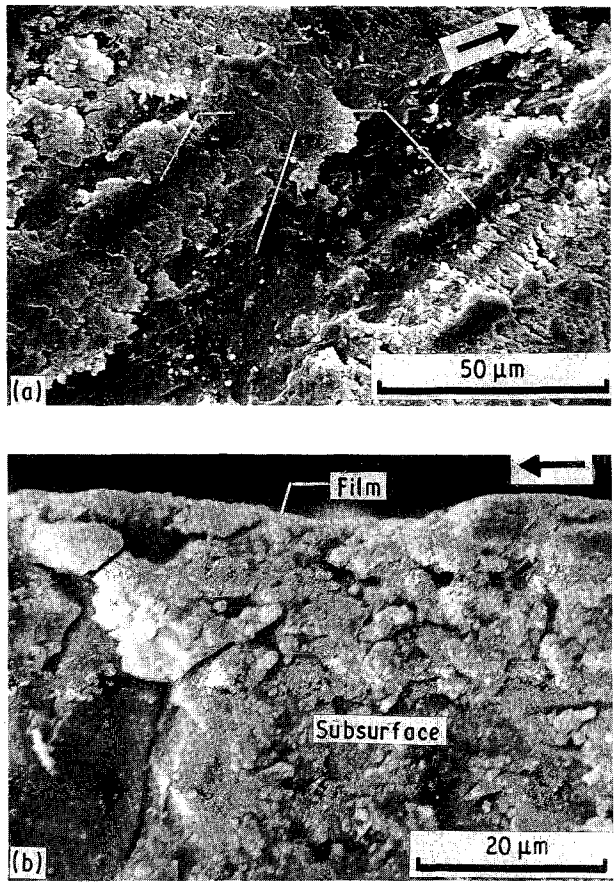

Figure 6 SEM micrographs (counterface roughness 0.05–0.1 μm CLA): (a) resin slid against steel at 2.04 MPa for 5 min and (b) parallel section of resin in steady state.

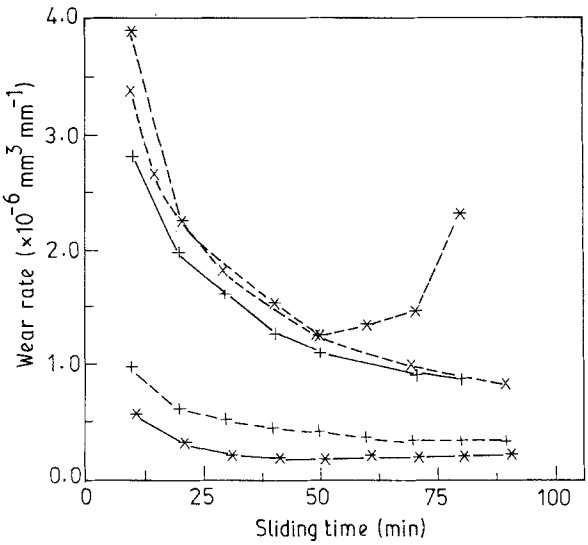

Figure 7 Wear rate against sliding time. Resin (counterface roughness 0.05–0.1 μm CLA): (*——*) normal pressure 4.25 MPa and (×——×) 2.04 MPa. Composite (4.25 MPa): (+——+) 1.0–1.5 μm CLA, and 0.05–0.1 μm CLA: (+——+) lubricated and (*——*) unlubricated.

formation of craters, which appears to destabilize an otherwise smooth film around the edge of the craters. As the cracks on the crater surface are directionally random, it is possible that they have been caused by localized regions of high hydrodynamic pressure.

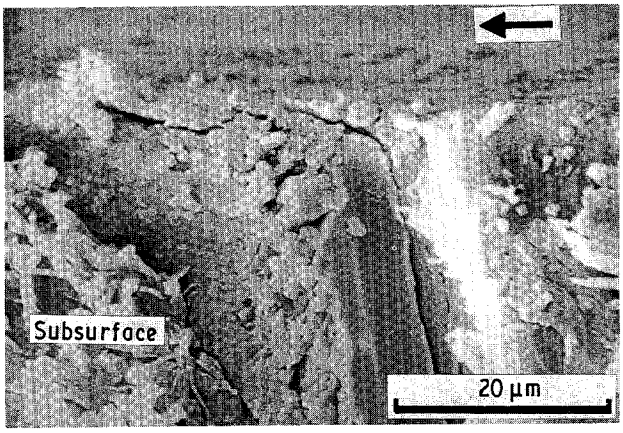

Figure 8 SEM of a parallel section of composite: normal pressure 2.04 MPa and counterface roughness 0.05–0.1 μm CLA.

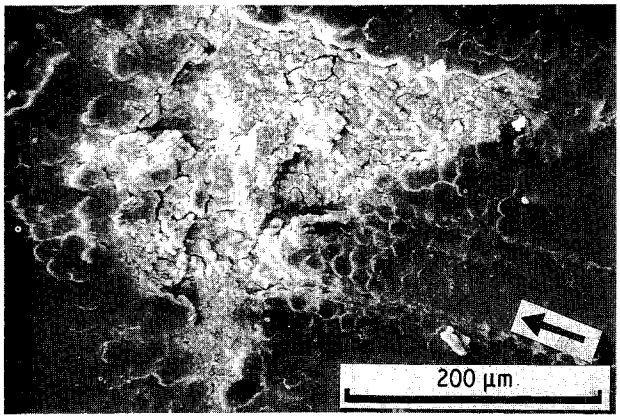

Figure 9 SEM of composite in the steady state: normal pressure 4.25 MPa and counterface roughness 0.05–0.1 μm CLA, water lubricated.

4. Discussion

In terms of mechanisms of friction and wear for the resin and the composite (up to a limiting pressure of about 4 MPa) there is a transient stage with respect to sliding time in which abrasion is the predominant mechanism. In this stage the coefficient of friction increases with the sliding time. As the debris is generated it is ironed on the surface to form polymer films, the role of which appears to be to take the process into a steady-state adhesion phase, especially as the counterface asperities become enveloped by the polymer film. The wear of these materials appears to be strongly influenced by the stability of these films. In the case of the resin high adhesion gives rise to stick–slip, which destabilizes the film and gives rise to a high wear rate. The addition of fibres to the resin arrests stick–slip and induces large plastic flow at the surface. This appears to stabilize the film, which now interacts with the counterface polymer film in a stable low-adhesion regime. The resultant wear is low. At normal pressures above 4 MPa both of the materials suffer wear due to surface melting.

Although the present study provides a phenomenological description of the process involved in the dry sliding of Kevlar–phenolic resin composite against steel, it raises two main questions that future studies will need to answer. First, why does the fibre addition lower the magnitude of adhesion at the interface sufficiently to change the polymer–steel interaction from stick–slip to ductile flow? Secondly, what role does the fibre play in providing stability to the film formed on the pin and the counterface surface? This issue is directly related to the wear of the composite. The present study suggests two possible roles. Fig. 10 shows a patch of film to be made up of debris compressed and oriented into a layered structure. Such films formed in the fibrous regions of the surface are likely to contain short fractured fibre ends or fibrils which, while in the film, will be oriented in the sliding direction. It is possible that this strengthens the film and makes it stable. Furthermore, the freshly frayed fibre ends can trap and anchor the debris, thus stabilizing the film. A patch of film held by a fibre end is seen in Fig. 11.

4.1. Application as a brake material

The high steady-state friction coefficient and poor wear resistance clearly render the resin a poor substitute for conventional brake materials such as asbestos.

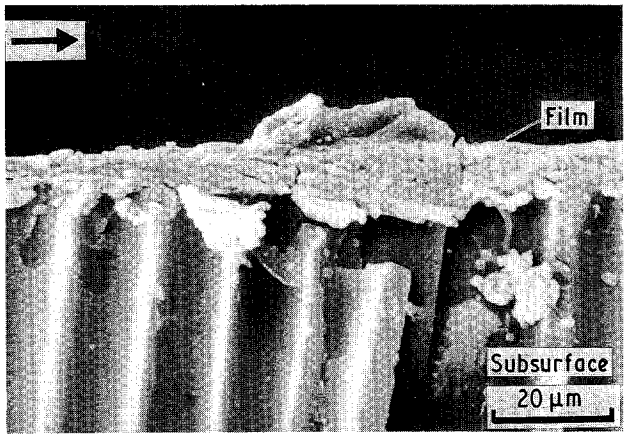

Figure 10 SEM of parallel section of composite: normal pressure 3.77 MPa and counterface roughness 0.05–0.1 μm CLA.

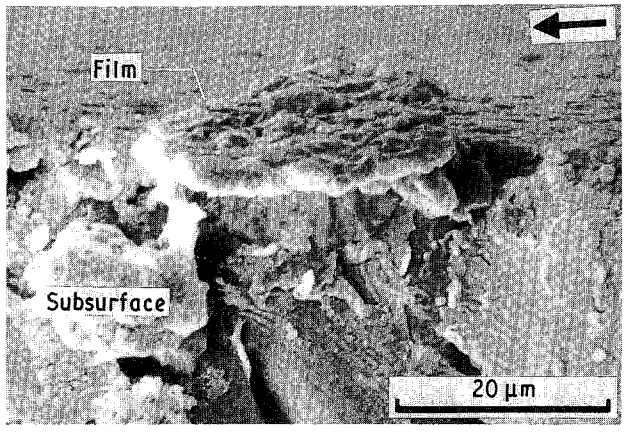

Figure 11 SEM of parallel section of composite: normal pressure 1.5 MPa and counterface roughness 0.05–0.1 μm CLA.

In the normal pressure range the addition of Kevlar fibres to the resin brings down the coefficient of friction closer to the acceptable range [3] but, more importantly, improves its wear resistance considerably. Furthermore, when water is present at the interface the friction coefficient is reduced but not so drastically as to render the composite useless as a brake material.

One of the important requirements of a brake material is that it should be able to generate high levels of friction quickly. In the light of this the present composite is seen to generate a high steady-state friction coefficient only at relatively long sliding times, although the gradient of coefficient of friction with time appears to increase with the normal pressure. Modification in the design of this composite is therefore required to enhance the rate at which stable polymer films are formed on the surface without sacrificing its excellent wear resistance.

5. Conclusion

A Kevlar–phenolic resin composite (30 wt % continuous Kevlar fibre) with the fibre axis normally oriented to the sliding plane was slid against EN24 steel discs at a constant velocity of 0.5 m s^{-1} in the pressure range 0.476–4.25 MPa. Phenomenological and morphological studies led to the following conclusions.

At short sliding times the composite is subjected to a predominantly ductile abrasion, whereas the resin suffers stick–slip and brittle failure in abrasion.

With further sliding the pin and the counterface both develop patches of film. When the surface is sufficiently covered by film, the interaction becomes adhesive and a steady-state stage of the process is reached. In the absence of fibre the polymer continues to exhibit stick–slip in the steady-state stage. This destabilizes the film while the compaction of the debris re-forms the film.

The adhesive forces in the absence of fibre is high. Addition of fibres lowers the steady-state friction coefficient from about 1.2–1.5 to 0.5–0.8.

The brittle response of the resin to traction and instability of the film on the pin give rise to a steady-state wear rate that is four times that of the composite. The trapping of debris by the frayed ends of the fibre appears to provide a stability to the film formed on the composite surface.

The tribological behaviour of the composite as noted in this study indicates its potential application as a brake material.

Acknowledgement

The authors are grateful for the useful discussions they had with Dr Kalyani Vijayan of National Aeronautical Laboratory, India.

References

1. M. CIRINO, R. B. PIPES and K. FRIEDRICH, *J. Mater. Sci.* **22** (1987) 2481.
2. C. LHYMN, K. E. TEMPELMLYER and P. K. DAVIS, *Composites* **16** (1985) 127.
3. B. J. BRISCOE, I. RAMIREZ and P. J. TWEEDLE, in Proceedings of the International Conference on Disc Brakes for Commercial Vehicles, London, 1–2 November 1988, The Institution of Mechanical Engineers (Mechanical Engineering Publication Ltd) p. 15.
4. J. BIJWE, U. S. TEWARI and P. VASUDEVAN, *Wear* **132** (1989) 247.
5. C. LHYMN and R. LIGHT, *ibid.* **116** (1987) 343.
6. H. VOSS and K. FRIEDRICK, *ibid.* **116** (1987) 1.
7. C. LHYMN, *ibid.* **114** (1987) 223.
8. K. FRIEDRICH and M. CYFFKA, *ibid.* **103** (1985) 333.
9. C. LHYMN, *Mater. Sci. Engng* **80** (1986) 93.
10. ZENG HANMIN, HE GUOREN and YANG GUICHENG, *Wear* **116** (1987) 59.
11. *Idem, ibid.* **116** (1987) 69.
12. T. TSUKIZOE and N. OHMAE, *Fibre Sci. Technol.* **18** (1983) 265.
13. C. LHYMN, *Wear* **122** (1988) 13.
14. R. RAMESH, KISHORE and R. M. V. G. K. RAO, *ibid.* **89** (1983) 131.

Received 13 February
and accepted 12 September 1991